Theriogenology 177 (2022) 11–21

Contents lists available at ScienceDirect

Theriogenology

journal homepage: www.theriojournal.com

WGBS combined with RNA-seq analysis revealed that Dnmt1 affects the methylation modification and gene expression changes during mouse oocyte vitrification

Yuzhen Ma [a, 1], Chunshen Long [b, 1], Gang Liu [c], Hongmei Bai [a], Lirong Ma [a], Taji Bai [a], Yongchun Zuo [b, **], Shubin Li [a, d, *]

[a] Centre of Reproductive Medicine, Inner Mongolia People's Hospital, Hohhot, Inner Mongolia, 010021, China
[b] The State Key Laboratory of Reproductive Regulation and Breeding of Grassland Livestock, College of Life Sciences, Inner Mongolia University, Hohhot, Inner Mongolia, 010020, China
[c] Key Laboratory of Medical Cell Biology, Clinical Medicine Research Center, Affiliated Hospital of Inner Mongolia Medical University, Tongdao North Street, Hohhot, 010050, Inner Mongolia, China
[d] Department of Geriatric Medical Center, Inner Mongolia People's Hospital, Hohhot, Inner Mongolia, 010021, China

ARTICLE INFO

Article history:
Received 22 April 2021
Received in revised form
28 September 2021
Accepted 29 September 2021
Available online 1 October 2021

Keywords:
Oocyte cryopreservation
DNA methylation
Gene expression
Gene regulatory network
Developmental ability
Fertilization potential

ABSTRACT

Understanding the molecular level changes of oocyte cryopreservation and the subsequent warming process is essential for improving the oocyte cryopreservation technologies. Here, we collected the mature metaphase II (MII) oocytes from mice and vitrified. After thawing, single-cell whole-genome bisulphite sequencing (scWGBS) and single-cell RNA sequencing (scRNA-seq) were used to investigate the molecular attributes of this process. Compared to the fresh oocytes, the vitrified oocytes had lower global methylation and gene expression levels, and 1426 genes up-regulated and 3321 genes down-regulated. The 1426 up-regulated differentially expressed genes (DEGs) in the vitrified oocytes were mainly associated with the histone ubiquitination, while the 3321 down-regulated genes were mainly enriched in the mitochondrion organisation and ATP metabolism processes. The differentially methylated regions (DMRs) were mainly located in promoter, intron and exon region of genes, and the length of DMRs in the vitrified oocytes were also significantly lower than that of the fresh oocytes. Notably, there were no significant difference in the expression levels of DNA demethylases (*Tet1*, *Tet2* and *Tet3*) and methyltransferases (*Dnmt3a* and *Dnmt3b*) between two treatments of oocytes. However, *Dnmt1* and *kcnq1ot1*, which are responsible for maintaining DNA methylation, were significantly down regulated in the vitrified oocytes. Gene regulatory network (GRN) analysis showed the *Dnmt1* and *kcnq1ot1* play a core role in regulating methylation and expression levels of downstream genes. Moreover, some genes associated with oocyte quality were significantly down-regulated in the vitrified oocytes. The present data provides a new perspective for understanding the impact of vitrification on oocytes.

1. Introduction

Oocyte cryopreservation (OC) is an important component of assisted reproductive technology (ART), which has been evolved and widely used [1]. And it is an effective method to preserve the fertility of women who lose ovarian function due to premature ovarian failure, pelvic disease, surgery, radiotherapy and chemotherapy [2–4]. In addition, there has been a shift in the timing of parenthood and more women are choosing to have children later in life [5]. With increasing age comes the natural decline in ovarian follicle number and quality of remaining oocytes, leading to the decreased female fertility and an increasing demand for OC [6].

In recent years, with the development of high-throughput sequencing technology, many studies have shown that the vitrification process can change the gene expression and epigenetic patterns of mammalian oocytes [7–9]. For example, Milroy et al. revealed that the global methylation levels in promoter regions of

* Corresponding author. Centre of Reproductive Medicine, Inner Mongolia People's Hospital, Hohhot, Inner Mongolia, 010021, China.
** Corresponding author.
E-mail addresses: yczuo@imu.edu.cn (Y. Zuo), lishubin033@163.com (S. Li).
[1] These authors have contributed equally to this work and share first authorship.

https://doi.org/10.1016/j.theriogenology.2021.09.032

Oct4 and *Sox2* in the vitrified oocytes were significantly lower than that of *in vivo* mature (IVM) mouse oocytes [10,11]. Cheng et al. found the methylation levels of three imprinted genes (*H19, Peg3 and Snrpn*) in blastocysts which are derived from mouse vitrified oocytes decreased [12]. In addition, the overall DNA methylation levels were also decreased in bovine vitrified MII oocytes [13,14]. At the same time, vitrification can also lead to the change of gene expression. For example, the expression levels of DNA methylation associated genes (*Dnmt1*, *Dnmt3a*, *Dnmt3b*, *Dnmt3l* and *Dnmt1o*), spindle assembly checkpoint (SAC)-related genes (*Mps1*, *BubR1*, *Mad1* and *Mad2*) and several imprinted genes (*Gtl2* and *Peg3*) were significantly down regulated in mouse vitrified oocytes [12,15–17]. However, whether the potential changes of gene expression and epigenetic pattern will have a negative impact on oocyte fertilization and subsequent embryonic development still needs further investigation.

As an epigenetic marker, DNA methylation plays an important role in maintaining parental imprinting and transcriptional regulation [7,18,19]. These genetic imprints are gradually established in the process of oocyte growth, which determines a large part of the genome DNA methylation profile of preimplantation embryos and influences the development of zygote, embryo, and postnatal life [20,21]. DNMT3A and DNMT3B are de novo methyltransferases, responsible for creating new methylation patterns [22–24]. DNMT3L lacks enzymatic activity, but enhances the activity of DNMT3A and DNMT3B [23]. Previous studies have shown that both *Dnmt3a*$^{-/-}$ and *Dnmt3l*$^{-/-}$ mice failed to establish germline methylation [25,26]. DNMT1 can catalyze de novo methylation of genes [27]. It is also a maintenance methyltransferase that copies pre-existing methylation patterns upon DNA replication, which is found in high abundance in growing oocytes and plays a role in maintaining methylation imprints during subsequent embryo cleavage [28,29]. And DNA demethylation mechanism is found to be mediated by the ten–eleven translocation (Tet) enzymes Tet1, Tet2, and Tet3 [30]. At present, whether vitrification will cause the expression patterns changes of these DNA methylation related enzymes, and then affect the methylation levels and gene expression patterns of oocytes remains poorly understood.

In this study, we used single-cell whole genome bisulphite sequencing (scWGBS) and single-cell RNA sequencing (scRNA-seq) to detect DNA methylation and gene expression changes in oocytes under cryopreservation treatment. The results revealed the lower DNA methylation level of the vitrified oocytes were associated with the down-regulated expression of Dnmt1 and Kcnq1ot1. At the same times, we found most of gene related to developmental and fertilization potential of oocytes were significant down-regulated in the vitrified oocytes. Our studies provided an in-depth understanding the effect of vitrification on oocytes.

2. Materials and methods

2.1. Animals

Female Institute of Cancer Research (ICR) mice at 6–8 weeks of age were purchased from SPF (Beijing, Biotechnology Co., Ltd.) and raised in a specific pathogen free environment employing a 12 h light/dark cycle, and a constant temperature (23 ± 1 °C) and humidity (60 ± 5%), respectively. All animal experiments were conformed to the ethics of the Institute of Zoology, Chinese Academy of Sciences.

2.2. Oocyte collection

To collect MII oocytes, the female ICR mice at 6–8 weeks of age were superovulated by the intraperitoneal injection with 10 U of pregnant mare serum gonadotropin (PMSG), followed by the intraperitoneal injection with 10 U of human chorionic gonadotropin (HCG). Cumulus oocyte complex (COC) were collected 12 h after HCG injection. Cumulus cells were digested with 0.2% hyaluronidase, and the denuded oocytes were transferred to the commercial M2 medium (Sigma, M7167, Shanghai, China).

The oocytes were microscopically observed and the oocytes with a polar body were defined as MII stage. After MII oocytes collection, the MII oocytes were randomly divide into a vitrification group and a fresh group. The fresh group directly subjected to subsequent RNA-seq and DNA methylation analyses. Vitrification group (n = 117) was used for subsequent vitrification experiments.

2.3. Oocyte vitrification and thawing

Commercial vitrification cryocoolant contained two types of vitrification medium as ES and VS was purchased from Vitrolife RapidVit™ Oocyte (Vitrolife,10121, Guangzhou, China). Before oocyte vitrification, a total of 1 mL of each solution was added into separate wells of a Vitrolife 4-well culture dish, and warmed at 37 °C. The denuded oocytes were transferred into the ES medium and incubated for 10 min. The oocytes were transferred to the VS medium with minimal volume to avoid dilution by a micropipette pre-primed with VS medium. Followed by incubation for 5 min, the oocytes were then transferred to a freezing rod, quickly put into liquid nitrogen, and kept vitrified for 30 days.

Commercial thawing liquid contained four types of thawing medium (TE, DS, WS1, and WS2), which was purchased from Vitrolife RapidWarm™ Oocyte (Vitrolife,10122, Guangzhou, China). Before oocyte thawing, a total of 1 mL of each medium was aliquoted into separate wells of a multi-well plate, and warmed at 37 °C. All manipulations of the oocytes were performed at 37 °C on a heated stage. The Vitrification System (Vitrolife Rapid-i) containing the vitrified oocytes was removed from the liquid nitrogen, and then collected the vitrified oocytes. The vitrified oocytes were immediately transferred into the TE medium for 1 min incubation, transferred into the DS medium for 3 min incubation, and finally transferred into the WS1 medium for 5 min incubation. Next, the oocytes were transferred into the WS2 media and incubated for 5–10 min, transferred to an equilibration solution with the plate placed in an incubator at 37 °C and 5% CO2 for 2 h. The equilibration solution in this study were TCM-199 medium (Thermo Fisher, 12350039, Shanghai, China) supplemented with 10% foetal bovine serum (Thermo Fisher, 30044333, Shanghai, China). Finally, we collected survival oocytes after vitrification and thawing for subsequent RNA-seq and DNA methylation analyses. Both the fresh group and the vitrified group contained three biological replicates, and each biological replicate contained ten oocytes.

2.4. Single-cell RNA-seq library construction, sequencing, and raw data processing

Single-cell RNA-seq library construction and sequencing were performed by Annoroad Gene Technology Co., Ltd (Beijing, China). The fresh oocytes and thawed vitrified oocytes were collected in tubes with lysis component and ribonuclease inhibitor. Then we carried out the amplification by the Smart-Seq2 method. An Oligo-dT primer was introduced to the reverse transcription reaction for first-strand cDNA synthesis, followed by PCR amplification to enrich the cDNA and magbeads purification step to clean up the production. Then the cDNA production was checked by Qubit® 3.0 Flurometer and Agilent 2100 Bioanalyzer to ensure the expected production with length around 1~2k bp. Then the cDNA was sheared randomly by ultrasonic waves for Illumina library preparation protocol. After library preparation, PerkinElmer LabChip®

GX Touch and Step OnePlus™ Real-Time PCR System were introduced for library quality inspection. Qualified libraries were then loaded on Illumina Hiseq platform for PE150 sequencing.

The number of raw reads was 42.1 million, and after quality control, 40.8 million clean reads were left. The original off-machine sequence (raw reads) obtained by HiSeq sequencing were filtered by the following steps to obtain the high-quality sequences (clean reads): (1) Removal of contaminated sequences and restriction sites in the reads (if the length of the reads is less than 30 bp after truncating the contaminated sequence, the reads were removed); (2) Removal of the reads containing adapters; (3) Removal of the low-quality reads (bases with a quality value of $Q \leq 19$ in the reads account for more than 50% of the total bases, for paired-end sequencing, if one end is low-quality, the reads at both ends were removed); (4) Removal of the reads with a ratio of N greater than 5% (for paired-end sequencing, if the ratio of N at one end was greater than 5%, the reads at both ends were removed). Next, the clean reads were aligned to the reference genome (mm9 assembly) using HISAT2 [31]. Then, the htseq-count was used to count the uniquely mapped reads [32].

2.5. DNA methylation library construction, sequencing, and raw data processing

Single-cell whole-genome bisulfite sequencing (scWGBS) was used to detect DNA methylation. The fresh and vitrified oocytes were used for this experiment. The fresh and thawed vitrified oocytes were lysed to separate their DNA, and unmethylated cytosines in the DNA fragment were converted to bisulphite, followed by the synthesis and PCR amplification of the first and second strands of DNA, to complete the single-cell double-strand library. Purified libraries were assessed for quality and quantity using Agilent Bioanalyzer and StepOnePlus Real-Time PCR System. Single cell libraries were prepared for 125 bp paired-end sequencing on a HiSeq2500.

After sequencing, the Trimmomatic (v0.36) software was used to filter the original sequence with the following steps: (1) Cut the sequence containing adapter with the following parameter: ILLUMINACLIP:Adapter.fa:2:30:10; (2) Use the sliding window method to trim the low-quality bases in reads with the following parameters: SLIDINGWINDOW: 4:15; (3) Cut off bases at both ends of reads whose quality value is less than three or N with parameter: LEADING: 3 TRAILING:3; (4) Discard reads with a length less than 36 nucleotides, after the trim, with the following parameters: MINLEN: 36. Finally, a clean high-quality data set was obtained. After data filtering, the clean reads were aligned to the reference genome (mm9 assembly) using Bismark (v0.16.3) [33]. The sequencing reads and the reference genome both underwent conversion of C-to-T and G-to-A. The converted reads were then aligned to the converted reference genome, and the best of four parallel comparison results was selected, and only comparison reads were used for subsequent analysis of methylation information. After the comparison quality was verified, these reads data that were uniquely aligned to the genome were used to obtain the cytosine methylation information, and perform the downstream DNA methylation information analysis.

2.6. Correlation analysis of the DNA methylation

To check the reproducibility of duplicate samples and compare the methylation differences between groups, the sliding window method (2 kb) was used to calculate the methylation levels in the whole genome, as well as the Pearson correlation coefficient of all samples [34]. The “methylation level” was determined by fraction of methylated cytosines, that is, methylated cytosines account for a proportion of all cytosine sites in the region.

2.7. Whole-genome and functional region methylation levels

To explore the methylation status of each sample in the whole gene range and compare the differences between groups, the overall methylation level of different samples was calculated using all methylated CpG sites. In order to understand the distribution of the window methylation level in the whole genome in detail, the methylation level of a 2 kb window of the whole gene was calculated. The violin diagrams were drawn to observe and compare the difference in the overall methylation level among different samples. We also evaluated the methylation levels in functional regions such as the promoter, untranslated region (UTR), coding sequence (CDS), intron, and intergenic regions, and displayed them with a boxplot.

2.8. Identification of differentially methylated regions (DMRs) and differentially expressed genes (DEGs)

Dispersion Shrinkage for Sequencing data (DSS) software [35] was used to identify DMRs. The regions with a p-value less than 0.05, average methylation level difference between groups greater than or equal to 0.2, and at least three CpG sites were retained as a final DMR. The differential expression analysis of genes was performed using DESeq2 [36,37]. Genes with $|\log2FC| \geq 1$ and adjusted p-value < 0.05 were identified as differentially expressed genes (DEGs).

2.9. Gene expression correlation analysis and UMAP dimensionality reduction

We used the logarithmic transformation (log2) to non-linearly normalise the read counts in the oocytes, followed by the calculation of Pearson correlation coefficient (PCC) between two kinds of oocytes, and the results were displayed in a heatmap. Regarding the UMAP dimensionality reduction analysis, we used the function “reduce_dimension” from the monocle3 package [38] of the R program, and the “plot_cells” function for visualisation.

2.10. Gene ontology (GO) and kyoto encyclopedia of genes and genomes (KEGG) pathway enrichment analyses

We performed GO and KEGG pathway enrichment analyses using clusterProfiler [39,40]. The function “enrich GO” and “enrich KEGG” with default parameters, were used for the GO terms and KEGG pathway enrichment analyses. Items with p-values < 0.05 were regarded as significantly enriched. The DEGs between the vitrified and fresh oocytes, and down-regulated expression genes with hypermethylated region (hyper-down) and up-regulated expression genes with hypomethylated region (hypo-up) were the input data of GO enrichment. The downstream genes of Dnmt1 were used to perform GO and KEGG enrichment.

2.11. Transcription factor (TF) associated gene regulatory network (GRN) analysis

The TF associated GRNs was generated by the R package SCENIC using the read count [41]. SCENIC is an algorithm that can reconstruct GRNs and identify stable cell states from single-cell RNA sequencing data (http://aertslab.org/#scenic). In short, SCENIC first inferred the co-expression modules and then trimmed them using *cis*-regulatory motif analyses, leaving a portion of the trimmed module, called the regulon. Next, SCENIC calculates the enrichment degree of each region by calculating the area under the restoration

curve (AUC) in the ranking of all genes for a specific region. We used a Z-score > 0.9 and importance value > 10 as the thresholds to select significant regulation modules.

2.12. Statistical analysis and data visualisation

The PCC was calculated using the "cor" function of R, with default parameters to estimate the correlation between genes [42]. Student's t-test was performed using the "t.test" function with default parameters [43,44].

In this study, data visualisation was mainly conducted by R (version 3.6.3), including the R/Bioconductor. The heatmap and Venn map were generated using Pheatmap and VennDiagram, respectively. The program ggpot2 (http://ggplot2.org/) was used to generate density plots, box plots and bubble plots.

3. Results

3.1. Significant global methylation and transcriptome differences were observed between the vitrified and fresh oocytes

To explore whether vitrification significantly affects methylation and gene expression in oocytes, we first calculated the PCCs between the fresh oocytes and vitrified oocytes based on methylation levels (fraction of methylated cytosines) and gene expression values (normalized read count), respectively (Fig. 1A and B). The results showed that there were high PCC value of methylation (PCC >0.85) and gene expression (PCC >0.9) among the oocytes under the same treatment, whereas there were obvious differences between the vitrified and fresh oocytes (methylation PCC <0.4 and gene expression PCC <0.9). The result of cell clusters based on gene expression also showed a high similarity among oocytes under the same treatment, and distinct differences between the vitrified and fresh oocytes (Fig. 1C).

Meanwhile, we found that the global methylation levels and gene expression levels of the vitrified oocytes were significantly lower than those of the fresh oocytes ($p < 0.001$) (Fig. 1D and E). In the exon, 3′ UTR and 5′ UTR regions, there were no significant difference in the methylation level between the vitrified and fresh oocytes. The methylation levels of intergenic, intron and promoter regions in the vitrified oocytes were significantly lower than those in the fresh oocytes ($p < 0.001$) (Fig. 1F). Overall, these results demonstrated that vitrification have significant effects on DNA methylation and gene expression pattern of oocytes.

3.2. Specific DNA methylation landscape and gene expression patterns between the vitrified and fresh oocytes

To further explore the effects of vitrification on the DNA methylation in oocytes, DSS software [31] was used to identify the differential methylation regions (DMRs) between the vitrified and fresh oocytes. And DMRs were annotated to various elements of genes, including CpG islands (CGIs), exons, introns, promoters, 3′ UTRs, and 5′ UTRs. The DEGs between the vitrified oocytes and fresh oocytes were identified by DEseq2. The genes with $|\log2FC| \geq 1$ and adjust p-value < 0.05 were identified as significantly DEGs.

The differential methylation analysis showed that the length of hypermethylated regions (the vitrified oocytes *vs.* the fresh oocytes) was shorter than that of hypomethylated regions, and the number of hypermethylated regions was less than that of hypomethylated regions in each gene region (Fig. 2A and B). These results suggested that the vitrification oocytes erased many of the wider methylation regions and reconstructed a small number of narrower methylation regions. The expression pattern of DEGs showed that the vitrified oocytes had a smaller number of up-regulated DEGs (n = 1426) than down-regulated DEGs (n = 3321) when compared to the fresh oocytes (Fig. 2C, Supplementary Table S1). The up-regulated DEGs in the vitrified oocytes were mainly enriched in the biological processes related to histone H2A monoubiquitination and polyubiquitination, endoplasmic reticulum tubular network organisation, and vesicle-mediated transport in synapses. The down-regulated DEGs in the vitrified oocytes were

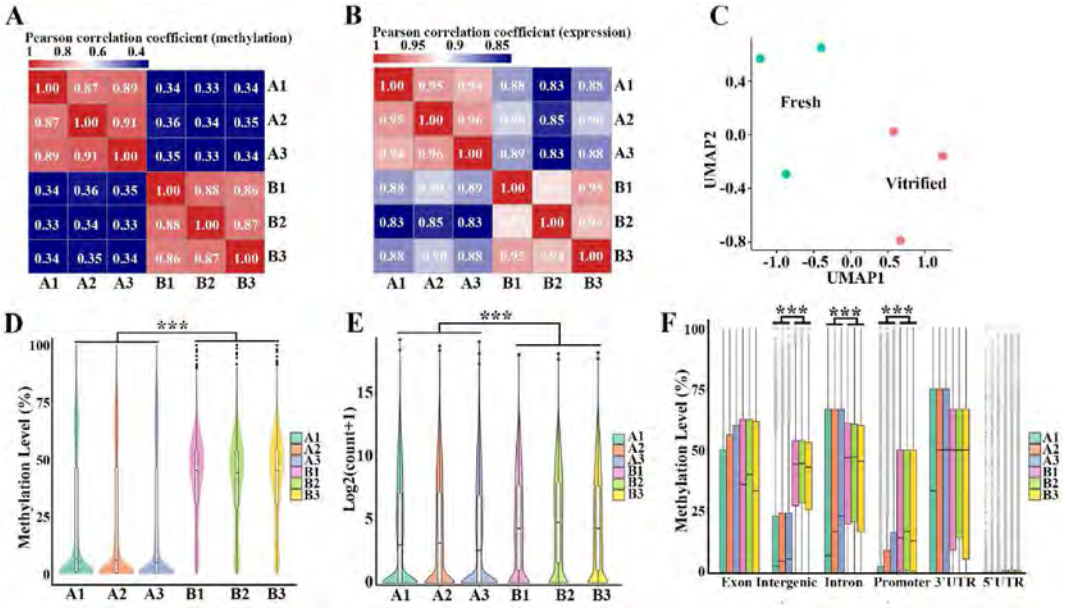

Fig. 1. The overall methylation and gene expression levels in the vitrified and fresh oocytes (A–B) The Pearson correlation of the methylation levels and gene expression levels between the vitrified oocytes (A1, A2, A3) and fresh oocytes (B1, B2, B3), respectively. **(C)** Uniform Manifold Approximation and Projection (UMAP) dimension reduction analysis of gene expression. Different cell types were labeled with different colours. **(D–E)** Violin diagrams show the differences in methylation and gene expression levels between the two treatments of oocytes. **(F)** The methylation level in different genome region of the genes. (For interpretation of the references to colour in this figure legend, the reader is referred to the Web version of this article.)

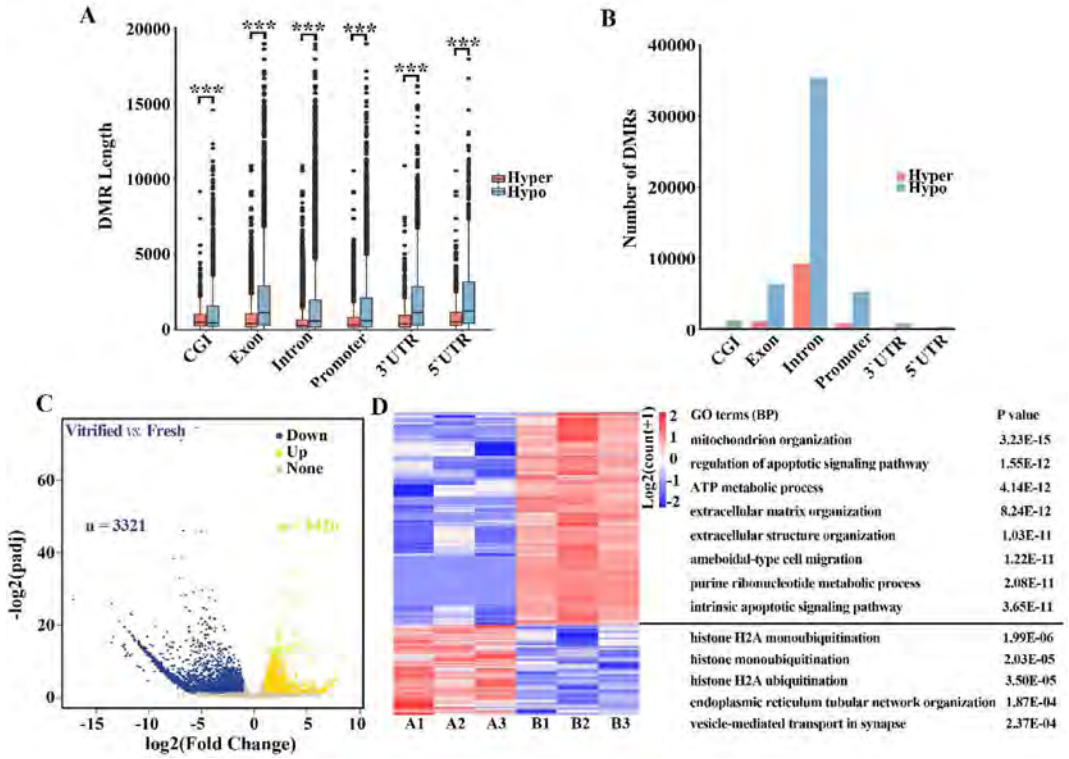

Fig. 2. The differential methylation regions (DMRs) and differentially expressed genes (DEGs) between the vitrified and fresh oocytes. (A–B) The length and the number of DMRs in each genomic element were significantly different (the vitrified oocytes *vs.* the fresh oocytes). Hypermethylated represented the regions where the methylation level in the vitrified oocytes were significantly higher than those of the fresh oocytes. Hypomethylated represented the regions where the methylation level in the vitrified oocytes were significantly lower than those of the fresh oocytes. **(C)** Volcano plot showed the DEGs (|log2FC| > 1, adjusted p-value < 0.05) between the vitrified oocytes and fresh oocytes. The vitrified oocytes have 1426 up-regulated and 3321 down-regulated DEGs compared to the fresh oocytes, respectively. **(D)** The expression patterns and GO terms (BP) of DEGs between the vitrified and fresh oocytes.

mainly enriched in some metabolic biological process, such as mitochondrial organisation, regulation of apoptotic signalling pathways, ATP metabolic processes, extracellular matrix organisation, extracellular structure organisation, and other biological processes (Fig. 2D). The above results indicated that the metabolic process in the fresh oocytes is obviously more active when compared to frozen oocytes. But chromatin structure and cytoskeleton structure were changed in frozen oocytes.

3.3. Gene expression related to methylation process in the vitrified and fresh oocytes

Considering that DNA methylation inhibit the binding of transcription factors and enhancer blocking elements, such as CTCF, thereby inhibiting gene expression [34], we performed a conjoint analysis of DNA methylation and the DEGs. The Manhattan plot shows a relatively even number of DMRs and DEGs among the 20 chromosomes in mouse oocytes (not included Y chromosome), indicating that vitrification treatment leads to the universal methylation and gene expression changes throughout the oocyte genome (Fig. 3A).

Surprisingly, 1285 DMRs were found, most of them were located in intergenic region, and only 97 DMRs regions were located in the promoter or gene body. Therefore, we combined these 97 CGI regions with the differential expression of the corresponding genes (Fig. 3B). The results showed the expression of eight genes, namely *Efna5*, *2310069G16Rik*, *1700030N03Rik*, *Mettl4*, *Naf1*, AU018091, *Popdc3*, and *Ethe1*, regulated by CGI differential methylation, were significantly up-regulated in the vitrified oocytes. The main biological processes of enrichment include the cell-cell adhesion mediated by integrin, regulation of presynaptic cytosolic calcium ion concentration, and lipoprotein localization. The hypermethylation of CGIs were associated with 19 genes including *Nxph4*, *Plekhh3*, *Sema4c*, *Rfx8*, *Tns2*, *Itga5*, *Phf10*, *C2*, *Foxp4*, *Lzts2*, *Adamtsl4*, *Unc119b*, *Hsd11b2*, *Ctxn1*, *Map1s*, *1810030O07Rik*, *Eef2kmt*, *Marcksl1*, and *Fbxl15*. The expression levels of these 19 genes were significantly down-regulated in the fresh oocytes. And these genes were involved in biological processes such as cellular responses to gonadotropic stimulus and follicle stimulating hormone (Fig. 3C). Although the global hyper-methylated CGIs were significantly narrower than those of the hypo-methylated CGIs (Fig. 2A), there was no significant difference (p-value > 0.05) in the width of differentially methylated CGIs which located in promoter or gene body regions (Fig. 3D).

In order to further study the mechanism of lower DNA methylation level in vitrification oocytes, we detected the expression patterns of DNA methylation-related enzymes (Fig. 3E). Although these genes contain many DMRs in the promoter and gene body regions (Fig. 3F), there were no significant difference in the expression levels of DNA demethylases (*Tet1*, *Tet2* and *Tet3*) and methyltransferases (*Dnmt3a* and *Dnmt3b*) between the vitrified and fresh oocytes. *Tet3* had a high expression level in both treatment of oocytes. Interestingly, Dnmt1, which is responsible for maintaining DNA methylation and catalyzing de novo methylation of genes, was significantly down-regulated in the vitrified oocytes. At the same time, the hyper-methylated DMRs of *Dnmt1* were more than that of Hypo-methylated DMRs. The expression of other genes seems to have little correlation with DNA methylation.

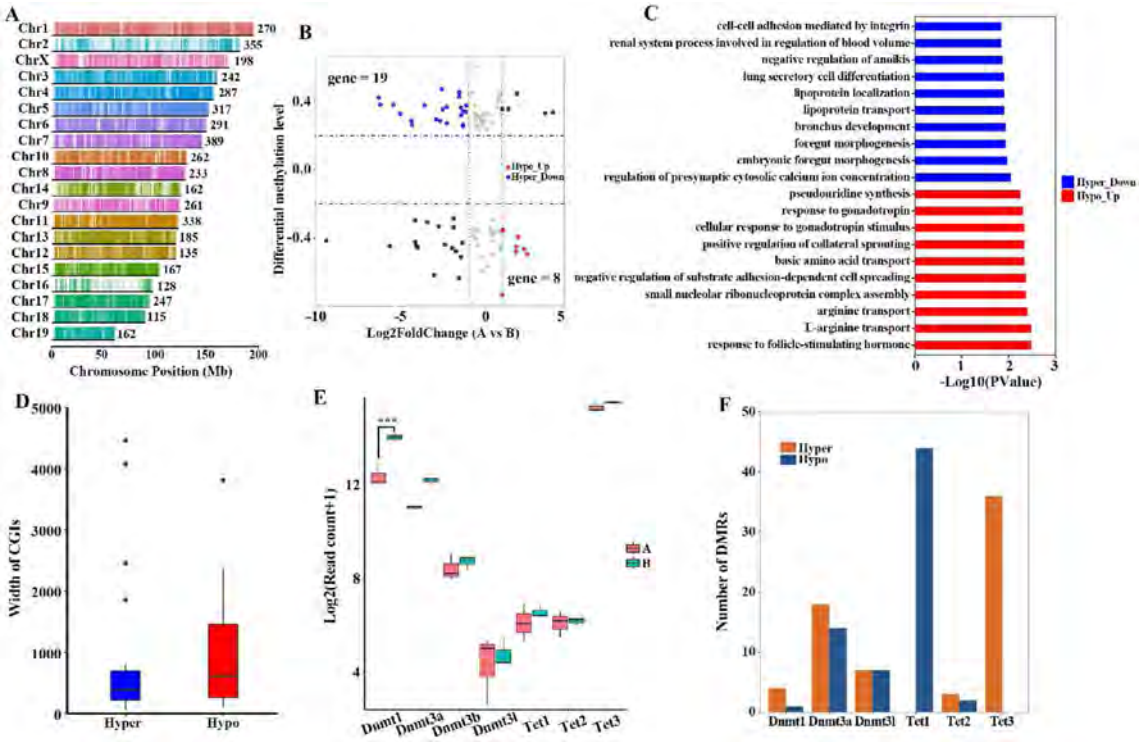

Fig. 3. Joint analysis between the DNA methylation and gene expression. (A) The Manhattan chart shows the distribution of DMRs and the number of DEGs on each chromosome. The number behind each chromosome indicates the number of DEGs. **(B)** The scatter plot shows the comparison between the DNA methylation and gene expression. Each dot represents a which was located in CGIs of promoter (or gene body) regions of gene. The hypermethylated DMRs of down-regulated genes (Hyper-Down) were labeled in blue, and the hypomethylated DMRs of up-regulated genes (Hypo-Up) were labeled in red. **(C)** GO terms enrichment of Hyper-Down and Hypo-Up genes, respectively. **(D)** The width of DMRs which located in CGIs of promoter and gene body regions. **(E)** The expression of genes that encoding DNA methylation-related enzymes. **(F)** The number of DMRs in the promoter and gene body regions of genes that encoding DNA methylation-related enzymes. (For interpretation of the references to colour in this figure legend, the reader is referred to the Web version of this article.)

3.4. The vitrified oocytes show GRN defects in maintaining DNA methylation

The above studies implied that the down-regulated expression of *Dnmt1* in the vitrified oocytes was associated with the lower overall DNA methylation levels observed in the vitrified oocytes. In order to further explore the reason for lower DNA methylation level in the vitrified oocytes, we evaluated the expression patterns of genes involved in the maintenance of DNA methylation, and found that *Kcnq1ot1* was also down-regulated in the vitrified oocytes. Next, we used the SCENIC [41] to detect the GRNs of *Dnmt1* and *Kcnq1ot1*. And the results revealed that the GRN of *Dnmt1* and *Kcnq1ot1* involved a total of 683 genes. The core network was composed of 21 genes, including *Dnmt1*, *Kcnq1ot1*, *Smad1*, *Sox5*, *Jazf1*, *Rfc2*, *Phf8*, *Nfkb2*, *Zbtb8b*, *Vezf1*, *Aff4*, *Rest*, *Arid5b*, *Cux1*, *Bptf*, *Dhx36*, *Rfxank*, *Crtc2*, *Atf4*, *Xrcc4*, and *Mterflb* (Fig. 4A). Among them, *Dnmt1* had 531 downstream target genes, and *Kcnq1ot1* was the downstream target gene of 51 TFs.

The results of GO enrichment indicated that the network involved in a series of biological processes, such as pattern specification process, regulation of binding, DNA-templated transcription, positive regulation of cell-cell adhesion, and negative regulation of binding (Fig. 4B). In addition, the enriched KEGG pathways included signalling pathways regulating pluripotency of stem cells, the MAPK signalling pathway, basal transcription factors, the Ras signalling pathway, as well as other key pathways (Fig. 4C). We counted the number of DMRs of these genes, and the results showed that the number of hypomethylation regions in the promoters, exons, introns, and 3′ UTR regions of these genes was significantly lower than that of hyper-methylation regions (p-value < 0.001) (Fig. 4D). Among the 683 genes in this TF-regulated network, 304 genes were differentially expressed between the vitrified and fresh oocytes. Among them, 214 genes (including *Dnmt1*) were down-regulated and 90 genes were up-regulated in the vitrified oocytes (Fig. 4E).

3.5. The vitrified oocytes exhibited a simpler GRN and developmental dysfunction

The transcriptional state of a cell emerges from its underlying gene regulatory network. To investigated the difference of underlying GRNs between the vitrified and fresh oocytes, the SCENIC [41] was used to perform further GRN analysis. In the vitrified oocytes, TFs such as *Rb1*, *Gm35315*, *Brf2*, and *Tbpl2* were core in the GRN (Fig. 5A). And TFs such as *Egr3*, *E2f1*, *Usf2*, *Lhx5*, *Kat2a*, *Foxp1*, and *Klf6* were core in the GRN of the fresh oocytes (Fig. 5B). The detailed GRNs of the vitrified oocytes and fresh oocytes were listed in Supplementary Table S2. There are more core TFs in GRN of the fresh oocytes compared to the vitrified oocytes. And the overall GRN is more complex, with more closely interactions among core TFs in the fresh oocytes. As expected, the core TFs of the vitrified and fresh oocytes were specifically expressed in respective oocytes (Fig. 5C).

Next, we assessed the developmental ability and fertilization potential of the vitrified oocytes. The expression of all genes in 101 GO terms related to oocytes quality and 34 GO terms related to fertilization were checked. The results revealed 10 GO terms related to oocyte quality and 10 GO terms related to fertilization contained

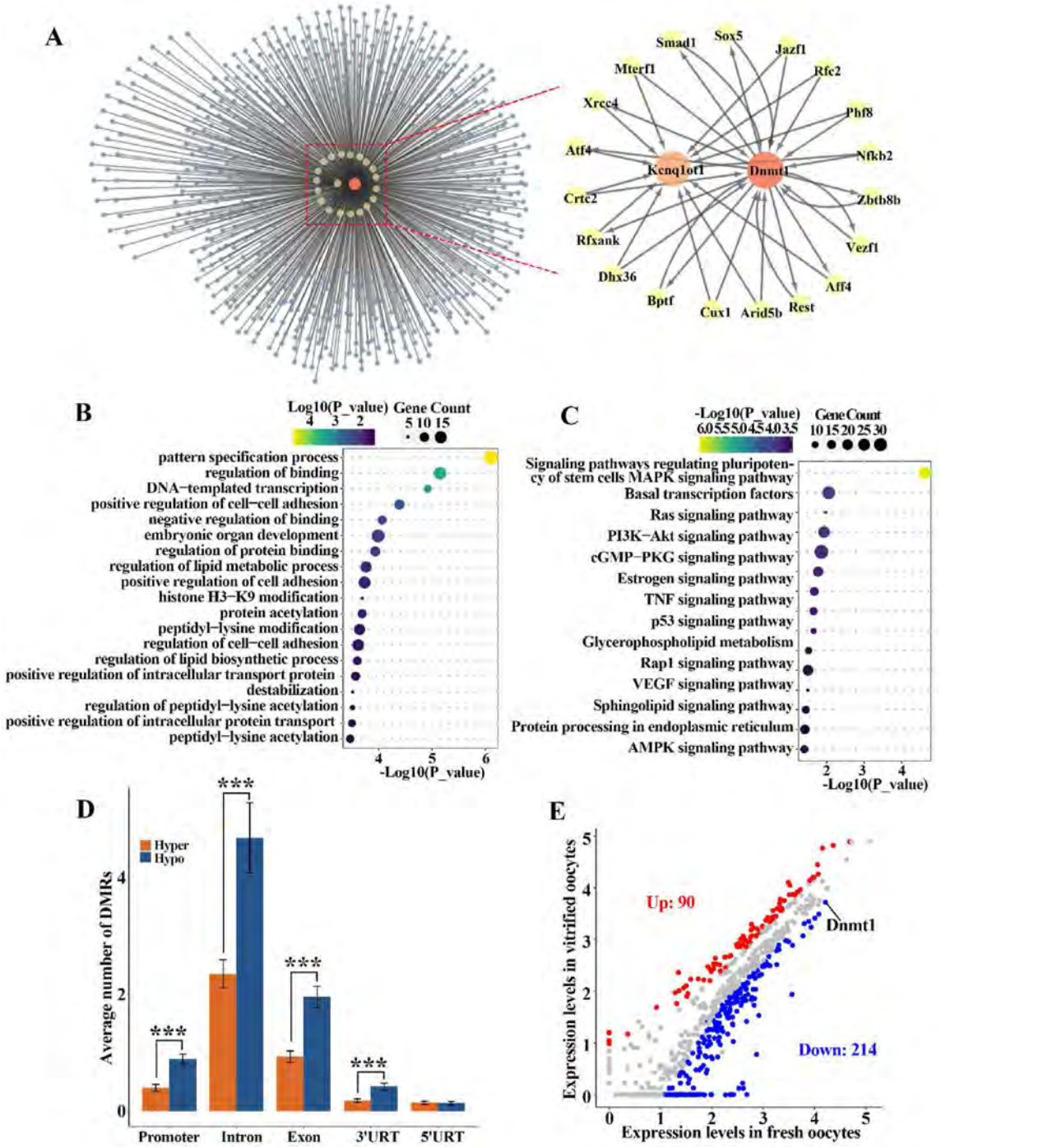

Fig. 4. Defective GRN related to maintain DNA methylation in the vitrified oocytes. (A) Based on SCENIC analysis, the GRN associated *Dnmt1* and *Kcnq1ot1* was showed. **(B–C)** GO and KEGG pathway enrichment analysis of genes in the GRN related to *Dnmt1* and *Kcnq1ot1*. **(D)** The average DMRs number of genes in the GRN associated with *Dnmt1* and *Kcnq1ot1*. Data are mean ± SEM (Standard Error of Mean). The p-value < 0.001 taken as being statistically significant using Student's t-test and denoted as ***. **(E)** The expression patterns of genes in the GRN associated with *Dnmt1* and *Kcnq1ot1*.

DEGs (Supplementary Table S3). The 10 GO terms related to oocytes quality includes oocyte development, oocyte maturation, ovulation, and so on, in which most of the DEGs were down-regulated in the vitrified oocytes (|log2FC| > 1, adjusted p-value < 0.05) (Fig. 5D). Similarly, most of the DEGs in fertilization related GO terms were down-regulated in the vitrified oocytes (|log2FC| > 1, adjusted p-value < 0.05) (Fig. 5E). These results suggest that vitrification treatment may cause some harm to developmental competence and fertilization potential of oocytes.

4. Discussion

The appearance of vitrification greatly improves the efficiency of oocyte preservation, which can protect the fertility of women at risk of medical or age-related fertility loss [7,45–47]. However, many studies have reported that oocyte vitrification could reduce

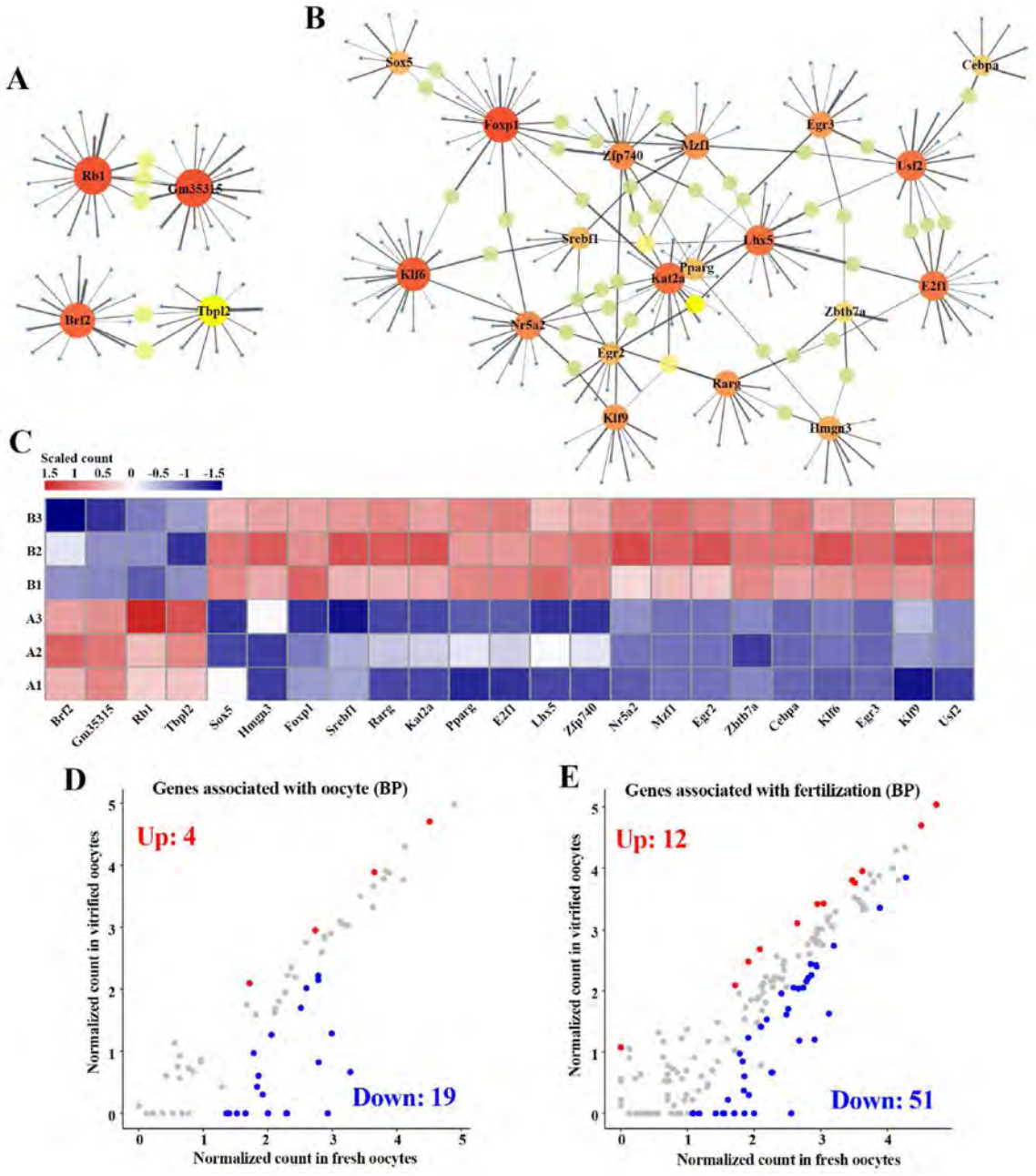

Fig. 5. Assessment of developmental and fertilization potential of the vitrified oocytes. (A–B) The most significant TF associated GRNs in the vitrified oocytes and fresh oocytes, respectively. The relationship between TFs and targets with Z-score > 0.9, importance >10 were retained. **(C)** The differential expression pattern of core TFs between the vitrified and fresh oocytes. **(D)** Differential expression of genes in 10 GO terms related to oocytes quality. **(E)** Differential expression of genes in 10 GO terms related to fertilization.

the potential for embryonic development in mammals in recent years [48–50]. The suboptimal cryovariables used for cryopreservation will cause cellular damage of oocytes occurring during cryopreservation. During the vitrification of oocytes, these cryovariables including type and concentration of cryoprotectant, nucleation temperature, cooling and thawing rates caused the cryoprotectant toxicity, intracellular ice crystals formation, subsequently results into DNA fragmentation, mRNA instability, free radical accumulation and ionic imbalances [51]. These abnormalities in oocytes disturbed the synthesis and preservation of transcripts, in particular expression of epigenetic modifier enzymes [52], further disturbing the translation and degradation of transcripts involved in epigenetic mechanisms required for meiotic progression, fertilization, and embryo development.

The effects of vitrification can be at the molecular level and influence epigenetic control and gene expression [53]. Monzo et al. found cryopreservation has a negative effect on gene expression profile of human MII oocytes. Moreover, many genes of ubiquitination pathway are down-regulated in the vitrified oocytes. The inhibition of this degradation mechanism may stabilize the maternal protein content necessary for oocyte development [54]. In bovine and pig oocytes, vitrification changes the expression patterns of many genes, including transcriptional regulation, cell differentiation and mitosis, actin cytoskeleton regulation and apoptosis pathway [55–57]. However, Gao et al. showed that there is no difference in gene expression between mouse vitrified and

fresh oocytes [58]. In our study, we performed scRNA-seq between the fresh and vitrified oocytes to detect the gene expression changes as the results of the vitrification. Our results showed that the global gene expression level of the vitrified oocytes is lower than that of the fresh oocytes ($p < 0.001$), and the vitrified oocytes have 1426 up-regulated DEGs and 3321 down-regulated DEGs compared to the fresh oocytes, respectively.

The up-regulated DEGs in the vitrified oocytes were mainly enriched in the biological processes that are associated with chromatin structure and cytoskeleton structure, such as histone H2A and histone monoubiquitination, endoplasmic reticulum tubular network organisation. Histone H2A ubiquitination plays an important role in many cellular events, such as transcription initiation and elongation, silencing, and DNA repair [59]. Distinct H2A ubiquitin ligases that mediate H2A ubiquitination are recruited based on the interactions with different corepressor complexes, and they contribute to the specific transcriptional repression programs [59]. The highly expressed genes that are enriched in histone ubiquitination and histone H2A ubiquitination may inhibit global gene expression in the vitrified oocytes. Meanwhile, the down-regulated DEGs were mainly enriched in mitochondrion organisation and metabolism processes. In mature oocytes, the mitochondrial size, function, and overall number are critical factors associated with successful fertilization and subsequent embryo development [60–62]. In addition, it is known that the mitochondrial network is highly vulnerable to temperature fluctuations. Our research also found that the expression levels of genes related mitochondrion organisation, ATP metabolic process in the vitrified oocytes was lower than that in the fresh oocytes. Therefore, it is beneficial to improve the quality of the vitrified oocytes by adding mitochondrial protective substances during vitrification.

Epigenetic information in the mammalian oocytes has the potential to be transmitted to the next generation and influence gene expression. Recent studies have shown that vitrification may alter the DNA methylation in mammalian oocytes, resulting in the abnormal embryo development [63–66]. On the other hand, some investigators found that there was no significant difference in DNA methylation status between the vitrified and control oocytes [67–69]. Our results showed that the global DNA methylation was decreased in the vitrified oocytes compared to the fresh oocytes. And 1285 DMRs were identified, most of which were located in the intergenic region and only 97 DMRs located in the promoter or gene body area. We also observed the expression of genes related to methylation. The genes which encode methyltransferases (*Dnmt3a*, *Dnmt3b*, *Dnmt3l*) and demethylases (*Tet1*, *Tet2*, and *Tet3*) were not differentially expressed between the fresh and vitrified oocytes. DNMT1 can catalyze de novo methylation of genes and is critical for producing competent oocytes and early embryos [27,29]. Therefore, the down-regulated of Dnmt1 may lead to abnormal genome-wide DNA methylation and poor embryo quality.

In conclusion, our results revealed the global effects of cryopreservation on the DNA methylation and gene expression patterns of oocytes and analyzed the changes of related biological process. We detected the expression patterns of DNA methylation-related enzymes and found *Dnmt1* were significantly down regulated in the vitrified oocytes. GRN analysis showed that the overall GRN is more complex, with more closely interactions among core TFs in the fresh oocytes. Through assessed the expression of genes that are associated with developmental ability and fertilization potential of oocytes, we found that vitrification treatment can cause some harm to developmental competence and fertilization potential of oocytes. Our study provided a new insight into understanding the effects of cryopreservation on oocytes at molecular level and provide a theoretical basis for improving the efficiency of oocyte cryopreservation.

Declaration of competing interest

The authors declare that the research was conducted in the absence of any commercial or financial relationships that could be construed as a potential conflict of interest.

CRediT authorship contribution statement

Yuzhen Ma: Conceptualization, Methodology, Writing – original draft. **Chunshen Long:** Formal analysis, Visualization, Writing – original draft. **Gang Liu:** Methodology. **Hongmei Bai:** Formal analysis. **Lirong Ma:** Methodology. **Taji Bai:** Methodology. **Yongchun Zuo:** Visualization, Writing – review & editing, Project administration, Conceptualization. **Shubin Li:** Project administration, Conceptualization.

CRediT authorship contribution statement

Yuzhen Ma: Conceptualization, Methodology, Writing – original draft. **Chunshen Long:** Formal analysis, Visualization, Writing – original draft. **Gang Liu:** Methodology. **Hongmei Bai:** Formal analysis. **Lirong Ma:** Methodology. **Taji Bai:** Methodology. **Yongchun Zuo:** Visualization, Writing – review & editing, Project administration, Conceptualization. **Shubin Li:** Project administration, Conceptualization.

Acknowledgments

We thank the financial support from the National Nature Scientific Foundation of China (grants 62061034, 61861036 and 82060567); Program for Young Talents of Science and Technology in Universities of Inner Mongolia Autonomous Region (grant NJYT-18-B01); and the Science and Technology Major Project of Inner Mongolia Autonomous Region of China to the State Key Laboratory of Reproductive Regulation and Breeding of Grassland Livestock (2019ZD031); Science and Technology Department of Inner Mongolia Autonomous Region, Science and Technology Achievement Transformation Project (CGZH2018178 and 2020BS08014); and Inner Mongolia Science and Technology Project, Maintenance and Reconstruction of Female Fertility (201502107).

Appendix A. Supplementary data

Supplementary data to this article can be found online at https://doi.org/10.1016/j.theriogenology.2021.09.032.

References

[1] Argyle CE, Harper JC, Davies MC. Oocyte cryopreservation: where are we now? Hum Reprod Update 2016;22:440–9.
[2] Abir R, Ben-Aharon I, Garor R, Yaniv I, Ash S, Stemmer SM, et al. Cryopreservation of in vitro matured oocytes in addition to ovarian tissue freezing for fertility preservation in paediatric female cancer patients before and after cancer therapy. Hum Reprod 2016;31:750–62.
[3] Liang T, Motan T. Mature oocyte cryopreservation for fertility preservation. Adv Exp Med Biol 2016;951:155–61.
[4] Johnston M, Richings NM, Leung A, Sakkas D, Catt S. A major increase in oocyte cryopreservation cycles in the USA, Australia and New Zealand since 2010 is highlighted by younger women but a need for standardized data collection. Hum Reprod 2020. Oxford, England.
[5] Mascarenhas M, Mehlawat H, Kirubakaran R, Bhandari H, Choudhary M. Live birth and perinatal outcomes using cryopreserved oocytes: an analysis of the Human Fertilisation and Embryology Authority database from 2000 to 2016 using three clinical models. Hum Reprod 2020. Oxford, England.
[6] Coello A, Pellicer A, Cobo A. Vitrification of human oocytes. Minerva Ginecol 2018;70:415–23.
[7] Barberet J, Barry F, Choux C, Guilleman M, Karoui S, Simonot R, et al. What impact does oocyte vitrification have on epigenetics and gene expression? Clin Epigenetics 2020;12:121.
[8] Buderatska N, Gontar J, Ilyin I, Lavrinenko S, Petrushko M, Yurchuk T. Does

human oocyte cryopreservation affect equally on embryo chromosome aneuploidy? Cryobiology 2020;93:33–6.
[9] Siano L, Engmann L, Nulsen J, Benadiva C. A prospective pilot study comparing fertilization and embryo development between fresh and vitrified sibling oocytes. Conn Med 2013;77:211–7.
[10] Milroy C, Liu L, Hammoud S, Hammoud A, Peterson CM, Carrell DT. Differential methylation of pluripotency gene promoters in in vitro matured and vitrified, in vivo-matured mouse oocytes. Fertility and sterility 2011;95:2094–9.
[11] Li H, Ta N, Long C, Zhang Q, Li S, liu S, et al. The spatial binding model of the pioneer factor Oct4 with its target genes during cell reprogramming. Computational and Structural Biotechnology Journal 2019;17:1226–33.
[12] Cheng KR, Fu XW, Zhang RN, Jia GX, Hou YP, Zhu SE. Effect of oocyte vitrification on deoxyribonucleic acid methylation of H19, Peg3, and Snrpn differentially methylated regions in mouse blastocysts. Fertility and sterility 2014;102:1183. 90.e3.
[13] Chen H, Zhang L, Deng T, Zou P, Wang Y, Quan F, et al. Effects of oocyte vitrification on epigenetic status in early bovine embryos. Theriogenology 2016;86:868–78.
[14] Hu W, Marchesi D, Qiao J, Feng HL. Effect of slow freeze versus vitrification on the oocyte: an animal model. Fertility and sterility 2012;98:752. 60.e3.
[15] Zhao XM, Ren JJ, Du WH, Hao HS, Wang D, Qin T, et al. Effect of vitrification on promoter CpG island methylation patterns and expression levels of DNA methyltransferase 1o, histone acetyltransferase 1, and deacetylase 1 in metaphase II mouse oocytes. Fertility and sterility 2013;100:256–61.
[16] Wu Z, Pan B, Qazi IH, Yang H, Guo S, Yang J, et al. Melatonin improves in vitro development of vitrified-warmed mouse germinal vesicle oocytes potentially via modulation of spindle assembly checkpoint-related genes. Cells 2019;8:1009.
[17] Chen H, Zhang L, Wang Z, Chang H, Xie X, Fu L, et al. Resveratrol improved the developmental potential of oocytes after vitrification by modifying the epigenetics. Mol Reprod Dev 2019;86:862–70.
[18] Greenberg MVC, Bourc'his D. The diverse roles of DNA methylation in mammalian development and disease. Nat Rev Mol Cell Biol 2019;20:590–607.
[19] Liu D, Li G, Zuo Y. Function determinants of TET proteins: the arrangements of sequence motifs with specific codes. Brief Bioinform 2019;20:1826–35.
[20] Smallwood SA, Tomizawa S, Krueger F, Ruf N, Carli N, Segonds-Pichon A, et al. Dynamic CpG island methylation landscape in oocytes and preimplantation embryos. Nat Genet 2011;43:811–4.
[21] Rutledge CE, Thakur A, O'Neill KM, Irwin RE, Sato S, Hata K, et al. Ontogeny, conservation and functional significance of maternally inherited DNA methylation at two classes of non-imprinted genes. Development 2014;141:1313–23.
[22] Bird A. DNA methylation patterns and epigenetic memory. Gene Dev 2002;16:6–21.
[23] Chen Z, Zhang Y. Role of mammalian DNA methyltransferases in development. Annu Rev Biochem 2020;89:135–58.
[24] Zuo YC, Song MM, Li HS, Chen X, Cao PB, Zheng L, et al. Analysis of the epigenetic signature of cell reprogramming by computational DNA methylation profiles. Curr Bioinform 2020;15:589–99.
[25] Kaneda M, Okano M, Hata K, Sado T, Tsujimoto N, Li E, et al. Essential role for de novo DNA methyltransferase Dnmt3a in paternal and maternal imprinting. Nature (London) 2004;429:900–3.
[26] Bourc'his D, Xu GL, Lin CS, Bollman B, Bestor TH. Dnmt3L and the establishment of maternal genomic imprints. Science 2001;294:2536–9.
[27] Bronner C, Alhosin M, Hamiche A, Mousli M. Coordinated dialogue between UHRF1 and DNMT1 to ensure faithful inheritance of methylated DNA patterns. Genes 2019;10.
[28] Uysal F, Ozturk S, Akkoyunlu G. DNMT1, DNMT3A and DNMT3B proteins are differently expressed in mouse oocytes and early embryos. Journal of molecular histology 2017;48:417–26.
[29] Hirasawa R, Chiba H, Kaneda M, Tajima S, Li E, Jaenisch R, et al. Maternal and zygotic Dnmt1 are necessary and sufficient for the maintenance of DNA methylation imprints during preimplantation development. Gene Dev 2008;22:1607–16.
[30] Moore LD, Le T, Fan G. DNA methylation and its basic function. Neuropsychopharmacology 2013;38:23–38.
[31] Kim D, Langmead B, Salzberg SL. HISAT: a fast spliced aligner with low memory requirements. Nat Methods 2015;12:357–60.
[32] Anders S, Pyl PT, Huber W. HTSeq–a Python framework to work with high-throughput sequencing data. Bioinformatics 2015;31:166–9.
[33] Krueger F, Andrews SR. Bismark: a flexible aligner and methylation caller for Bisulfite-Seq applications. Bioinformatics 2011;27:1571–2.
[34] Li H, Long C, Xiang J, Liang P, Li X, Zuo Y. Dppa2/4 as a trigger of signaling pathways to promote zygote genome activation by binding to CG-rich region. Brief Bioinform 2020.
[35] Feng H, Conneely KN, Wu H. A Bayesian hierarchical model to detect differentially methylated loci from single nucleotide resolution sequencing data. Nucleic Acids Res 2014;42:e69.
[36] Wang L, Feng Z, Wang X, Wang X, Zhang X. DEGseq: an R package for identifying differentially expressed genes from RNA-seq data. Bioinformatics 2010;26:136–8.
[37] Long CS, Li W, Liang PF, Liu S, Zuo YC. Transcriptome comparisons of multi-species identify differential genome activation of mammals embryogenesis. Ieee Access 2019;7:7794–802.
[38] Cao J, Spielmann M, Qiu X, Huang X, Ibrahim DM, Hill AJ, et al. The single-cell transcriptional landscape of mammalian organogenesis. Nature (London) 2019;566:496–502.
[39] Yu G, Wang LG, Han Y, He QY. clusterProfiler: an R package for comparing biological themes among gene clusters. OMICS 2012;16:284–7.
[40] Wang H, Liang P, Zheng L, Long C, Li H, Zuo Y. eHSCPr discriminating the cell identity involved in endothelial to hematopoietic transition. Bioinformatics 2021. Oxford, England.
[41] Aibar S, Gonzalez-Blas CB, Moerman T, Huynh-Thu VA, Imrichova H, Hulselmans G, et al. SCENIC: single-cell regulatory network inference and clustering. Nat Methods 2017;14:1083–6.
[42] Ahlgren P, Jarneving B, Rousseau R. Requirements for a cocitation similarity measure, with special reference to Pearson's correlation coefficient. J Am Soc Inf Sci Technol 2003;54:550–60.
[43] Bandyopadhyay S, Mallik S, Mukhopadhyay A. A survey and comparative study of statistical tests for identifying differential expression from microarray data. IEEE ACM Trans Comput Biol Bioinf 2014;11:95–115.
[44] Greenland S, Senn SJ, Rothman KJ, Carlin JB, Poole C, Goodman SN, et al. Statistical tests, P values, confidence intervals, and power: a guide to misinterpretations. Eur J Epidemiol 2016;31:337–50.
[45] Mature oocyte cryopreservation: a guideline. Fertility and sterility 2013;99:37–43.
[46] Stoop D, van der Veen F, Deneyer M, Nekkebroeck J, Tournaye H. Oocyte banking for anticipated gamete exhaustion (AGE) is a preventive intervention, neither social nor nonmedical. Reprod Biomed Online 2014;28:548–51.
[47] Fertility preservation in patients undergoing gonadotoxic therapy or gonadectomy: a committee opinion. Fertility and sterility 2013;100:1214–23.
[48] Kohaya N, Fujiwara K, Ito J, Kashiwazaki N. Generation of live offspring from vitrified mouse oocytes of C57BL/6J strain. PloS one 2013;8:e58063.
[49] Zhao XM, Hao HS, Du WH, Zhao SJ, Wang HY, Wang N, et al. Melatonin inhibits apoptosis and improves the developmental potential of vitrified bovine oocytes. J Pineal Res 2016;60:132–41.
[50] Zuo Y, Gao Y, Su G, Bai C, Wei Z, Liu K, et al. Irregular transcriptome reprogramming probably causes thec developmental failure of embryos produced by interspecies somatic cell nuclear transfer between the Przewalski's gazelle and the bovine. BMC Genom 2014;15:1113.
[51] Chatterjee A, Saha D, Niemann H, Gryshkov O, Glasmacher B, Hofmann N. Effects of cryopreservation on the epigenetic profile of cells. Cryobiology 2017;74:1–7.
[52] Christou-Kent M, Dhellemmes M, Lambert E, Ray PF, Arnoult C. Diversity of RNA-binding proteins modulating post-transcriptional regulation of protein expression in the maturing mammalian oocyte. Cells 2020;9.
[53] Barberet J, Barry F, Choux C, Guilleman M, Karoui S, Simonot R, et al. What impact does oocyte vitrification have on epigenetics and gene expression? Clin Epigenetics 2020;12:121.
[54] Monzo C, Haouzi D, Roman K, Assou S, Dechaud H, Hamamah S. Slow freezing and vitrification differentially modify the gene expression profile of human metaphase II oocytes. Hum Reprod 2012;27:2160–8.
[55] Huang J, Ma Y, Wei S, Pan B, Qi Y, Hou Y, et al. Dynamic changes in the global transcriptome of bovine germinal vesicle oocytes after vitrification followed by in vitro maturation. Reproduction, fertility, and development 2018;30:1298–313.
[56] Wang N, Li CY, Zhu HB, Hao HS, Wang HY, Yan CL, et al. Effect of vitrification on the mRNA transcriptome of bovine oocytes. Reproduction in domestic animals = Zuchthygiene 2017;52:531–41.
[57] Jia BY, Xiang DC, Quan GB, Zhang B, Shao QY, Hong QH, et al. Transcriptome analysis of porcine immature oocytes and surrounding cumulus cells after vitrification and in vitro maturation. Theriogenology 2019;134:90–7.
[58] Gao L, Jia G, Li A, Ma H, Huang Z, Zhu S, et al. RNA-Seq transcriptome profiling of mouse oocytes after in vitro maturation and/or vitrification. Sci Rep 2017;7:13245.
[59] Zhou W, Wang X, Rosenfeld MG. Histone H2A ubiquitination in transcriptional regulation and DNA damage repair. The international journal of biochemistry & cell biology 2009;41:12–5.
[60] Lei T, Guo N, Tan MH, Li YF. Effect of mouse oocyte vitrification on mitochondrial membrane potential and distribution. J Huazhong Univ Sci Technolog Med Sci 2014;34:99–102.
[61] Liang Y, Ning FY, Du WJ, Wang CS, Piao SH, An TZ. The type and extent of injuries in vitrified mouse oocytes. Cryobiology 2012;64:97–102.
[62] Szurek EA, Eroglu A. Comparison and avoidance of toxicity of penetrating cryoprotectants. PloS one 2011;6:e27604.
[63] Xu BF, Liu DY, Wang ZR, Tian RX, Zuo YC. Multi-substrate selectivity based on key loops and non-homologous domains: new insight into ALKBH family. Cell Mol Life Sci 2021;78:129–41.
[64] Wang Z, Liu D, Xu B, Tian R, Zuo Y. Modular arrangements of sequence motifs determine the functional diversity of KDM proteins. Brief Bioinform 2020.
[65] Hanna CW, Hannah D, Gavin K. Epigenetic regulation in development: is the mouse a good model for the human? Hum Reprod Update 2018.
[66] Sendikait G, Kelsey G. The role and mechanisms of DNA methylation in the oocyte. Essays Biochem 2019;63.

[67] Fu L, Chang H, Wang Z, Xie X, Quan F. The effects of TETs on DNA methylation and hydroxymethylation of mouse oocytes after vitrification and warming. Cryobiology 2019;90.
[68] Jie Y, Zhang L, Wang T, Rong L, Jie Q. Effect of vitrification at the germinal vesicle stage on the global methylation status in mouse oocytes subsequently matured in vitro. Chin Med J (Taipei) 2014;127:4019–24.
[69] Chen H, Zhang L, Wang Z, Chang H, Xie X, Fu L, et al. Resveratrol improved the developmental potential of oocytes after vitrification by modifying the epigenetics. Molecular reproduction and development; 2019.